Molecular Phylogenetics and Evolution 50 (2009) 642–653

Contents lists available at ScienceDirect

Molecular Phylogenetics and Evolution

journal homepage: www.elsevier.com/locate/ympev

A multi-locus time-calibrated phylogeny of the siphonous green algae

Heroen Verbruggen [a,*], Matt Ashworth [b], Steven T. LoDuca [c], Caroline Vlaeminck [a], Ellen Cocquyt [a], Thomas Sauvage [d], Frederick W. Zechman [e], Diane S. Littler [f], Mark M. Littler [f], Frederik Leliaert [a], Olivier De Clerck [a]

[a] Phycology Research Group and Center for Molecular Phylogenetics and Evolution, Ghent University, Krijgslaan 281, Building S8, 9000 Ghent, Belgium
[b] Section of Integrative Biology, University of Texas at Austin, 1 University Station MS A6700, Austin, TX 78712, USA
[c] Department of Geography and Geology, Eastern Michigan University, Ypsilanti, MI 48197, USA
[d] Botany Department, University of Hawaii at Manoa, 3190 Maile Way, Honolulu, HI 96822, USA
[e] Department of Biology, California State University at Fresno, 2555 East San Ramon Avenue, Fresno, CA 93740, USA
[f] Department of Botany, National Museum of Natural History, Smithsonian Institution, Washington, DC 20560, USA

ARTICLE INFO

Article history:
Received 4 November 2008
Revised 15 December 2008
Accepted 18 December 2008
Available online 25 December 2008

Keywords:
Molecular phylogenetics
Relaxed molecular clock
Fossil algae
Bryopsidales
Dasycladales
Ulvophyceae
Chlorophyta

ABSTRACT

The siphonous green algae are an assemblage of seaweeds that consist of a single giant cell. They comprise two sister orders, the Bryopsidales and Dasycladales. We infer the phylogenetic relationships among the siphonous green algae based on a five-locus data matrix and analyze temporal aspects of their diversification using relaxed molecular clock methods calibrated with the fossil record. The multi-locus approach resolves much of the previous phylogenetic uncertainty, but the radiation of families belonging to the core Halimedineae remains unresolved. In the Bryopsidales, three main clades were inferred, two of which correspond to previously described suborders (Bryopsidineae and Halimedineae) and a third lineage that contains only the limestone-boring genus *Ostreobium*. Relaxed molecular clock models indicate a Neoproterozoic origin of the siphonous green algae and a Paleozoic diversification of the orders into their families. The inferred node ages are used to resolve conflicting hypotheses about species ages in the tropical marine alga *Halimeda*.

© 2008 Elsevier Inc. All rights reserved.

1. Introduction

The siphonous green algae form a morphologically diverse group of marine macroalgae. They are readily distinguished from other green algae by their ability to form large, differentiated thalli comprised of a single, giant tubular cell. This tubular cell branches and fuses in various patterns to form a broad range of forms (Fig. 1). Individual branches of the tubular cell are called siphons. The siphonous green algae include two sister orders (Bryopsidales and Dasycladales) and belong to the chlorophytan class Ulvophyceae. The Cladophorales, an order closely related to the Bryopsidales and Dasycladales (Zechman et al., 1990), is sometimes included in the siphonous algae but its members are not truly siphonous because they are generally multicellular. The siphonous green algae are unique among their chlorophytan relatives in having a relatively rich fossil record because many of them biomineralize.

The Bryopsidales range in morphology from simple, branched thalli (Fig. 1A and B) to more complex organizations with interwoven siphons, differentiated thalli and various morpho-ecological specializations (Fig. 1C–F). They have multiple nuclei scattered throughout the siphons. These algae form an important component of the marine flora, particularly in tropical marine environments, where they are among the major primary producers on coral reefs, in lagoons and seagrass beds. They comprise roughly 500 recognized species (Guiry and Guiry, 2008). The calcified representatives are major contributors of limestone to coral reef systems and are well-represented in the fossil record (Hillis-Colinvaux, 1986; Mu, 1990). The Bryopsidales are also common in warm-temperate marine habitats where they form a significant component of the flora (e.g., *Codium*). Several bryopsidalean taxa are vigorous invasive species (e.g., *Codium fragile*, *Caulerpa taxifolia* and *Caulerpa racemosa* var. *cylindracea*) that are known to have profoundly affected the ecology and native biota in areas of introduction. Molecular phylogenetic studies have shown two principal bryopsidalean lineages, both comprising simple as well as complex forms (Lam and Zechman, 2006; Verbruggen et al., 2009; Woolcott et al., 2000).

Extant Dasycladales are characterized by a central axis surrounded by whorls of lateral branches (Fig. 1G–J). Members of this group contain a single giant nucleus situated in the rhizoid during

* Corresponding author. Fax: +32 9 264 8599.
E-mail addresses: heroen.verbruggen@ugent.be (H. Verbruggen), mashworth@mail.utexas.edu (M. Ashworth), steve.loduca@emich.edu (S.T. LoDuca), caroline.vlaeminck@ugent.be (C. Vlaeminck), ellene.cocquyt@ugent.be (E. Cocquyt), sauvage@hawaii.edu (T. Sauvage), zechman@csufresno.edu (F.W. Zechman), littlerd@si.edu (D.S. Littler), littlerm@si.edu (M.M. Littler), frederik.leliaert@ugent.be (F. Leliaert), olivier.declerck@ugent.be (O. De Clerck).

1055-7903/$ - see front matter © 2008 Elsevier Inc. All rights reserved.
doi:10.1016/j.ympev.2008.12.018

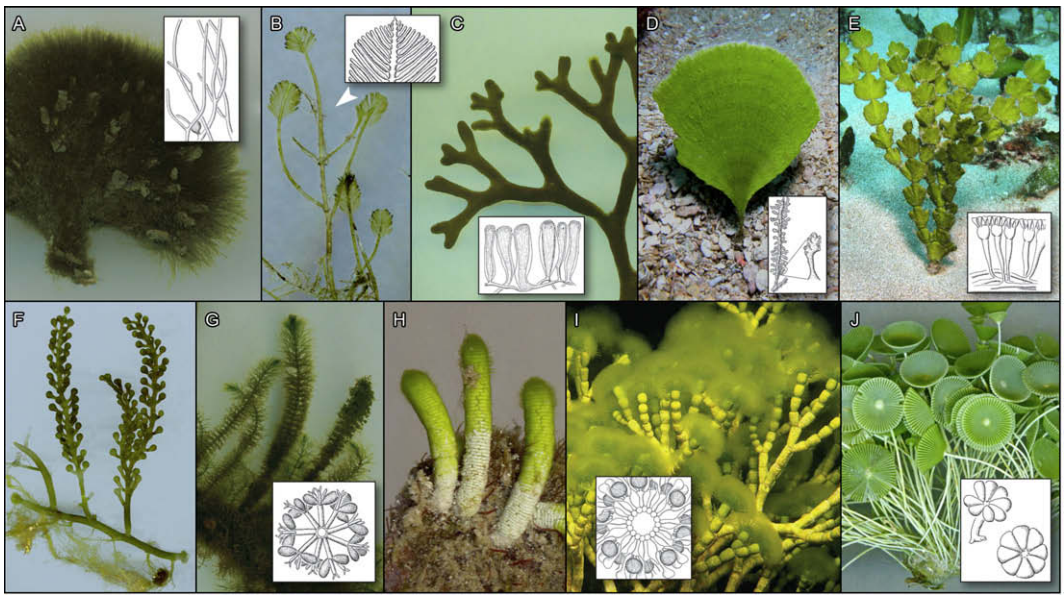

Fig. 1. Morphology and anatomy of the siphonous green algae comprising the orders Bryopsidales (A–F) and Dasycladales (G–J). (A) *Derbesia*, (B) *Bryopsis*, (C) *Codium*, (D) *Udotea*, (E) *Halimeda*, (F) *Caulerpa*, (G) *Batophora*, (H) *Neomeris*, (I) *Cymopolia*, (J) *Acetabularia*.

the vegetative phase of their life cycle. Albeit relatively inconspicuous, they are common algae of shallow tropical and subtropical marine habitats. Both calcified and non-calcified representatives have left a rich fossil record dating back to the Cambrian Period (540–488 my) (Berger and Kaever, 1992; LoDuca et al., 2003). Fossil remains suggest that non-calcified dasyclads were most diverse during the Ordovician and Silurian periods and declined in favor of calcified representatives after the Early Devonian (±400 my), perhaps as a result of selection for resistance to herbivory (LoDuca et al., 2003). In all, over 700 species are known from the fossil record, and fossil dasyclads are important tools for both biostratigraphic and paleoenvironmental studies (Berger and Kaever, 1992; Bucur, 1999). The present dasycladalean diversity consists of 37 species belonging to 10 genera and the two families Dasycladaceae and Polyphysaceae (Berger, 2006). Molecular phylogenetic studies have shown that the Polyphysaceae arose from the Dasycladaceae, leaving the latter paraphyletic (Berger et al., 2003; Olsen et al., 1994; Zechman, 2003).

Currently available phylogenetic studies of the siphonous green algae suffer from a few shortcomings. First, the studies have been based on single loci, yielding partially resolved trees with some unresolved taxa. Second, several important groups within the Bryopsidales have not been included. Finally, the temporal aspects of siphonous green algal diversification have not been explored in sufficient detail. Several recent studies point to the necessity of a time-calibrated phylogenetic framework. For example, the large discrepancy between species ages resulting from interpretations of molecular data and the fossil record creates confusion (Dragastan et al., 2002; Kooistra et al., 2002). Furthermore, biogeographic interpretations are difficult without reference to a temporal framework (Verbruggen et al., 2005, 2007). So far, the fossil record has been used on one occasion to calibrate a dasycladalean molecular phylogeny in geological time (Olsen et al., 1994). In the years that have passed since the publication of this study, however, several important discoveries have been made in dasyclad paleontology (e.g., Kenrick and Li, 1998; LoDuca et al., 2003) and more advanced calibration methods have been developed (reviewed by e.g., Verbruggen and Theriot, 2008).

The present study sets out to achieve two goals. First, it aims to resolve the phylogeny of the siphonous green algae more fully and include previously omitted taxonomic groups. Second, it aspires to provide a temporal framework of siphonous green algal diversification by calibrating the phylogeny in geological time using information from the fossil record. Our approach consists of model-based phylogenetic analyses of a five-locus alignment spanning both of the orders and uses a composite (partitioned) model of sequence evolution. Calibration of the phylogeny in geological time is achieved with Bayesian implementations of relaxed molecular clock models, using a selection of fossil reference points.

2. Materials and methods

2.1. Data generation

In preparation for this study, the *rbc*L gene of a wide spectrum of taxa was sequenced as described below and additional *rbc*L sequences were downloaded from GenBank. From a neighbor joining guide tree produced from these sequences, 56 taxa representing all major clades were selected. For these taxa, we attempted to amplify four additional loci (plastid encoding *atp*B, *tuf*A and 16S rDNA, and nuclear 18S rDNA) or downloaded this information from GenBank.

DNA extraction followed a CTAB protocol modified from Doyle and Doyle (1987). DNA amplification followed previously published protocols (Famà et al., 2002; Hanyuda et al., 2000; Karol et al., 2001; Kooistra, 2002; Lam and Zechman, 2006; Olson et al., 2005; Wolf, 1997), with additional primers for amplification of partial sequences of the *rbc*L gene and the 16S rDNA. A complete overview of the primers used is given in Fig. 2. Newly generated sequences were submitted to GenBank. A complete list of Genbank accession numbers is provided in Table 1. Our specimens are vouchered in the Ghent University Herbarium or the US National Herbarium (see GenBank records for voucher information). The ulvophycean algae *Trentepohlia aurea*, *Oltmannsiellopsis viridis*, *Ulva intestinalis*, *Ulothrix zonata* and *Pseudendoclonium akinetum* were used as outgroup taxa (Lopez-Bautista and Chapman, 2003). Despite the fact that the order Cladophorales is the closest relative of Bryopsidales and Dasycladales (Zechman et al., 1990), we did not use it as an outgroup because it has proven impossible to amplify chloroplast DNA in its members using standard primer combinations.

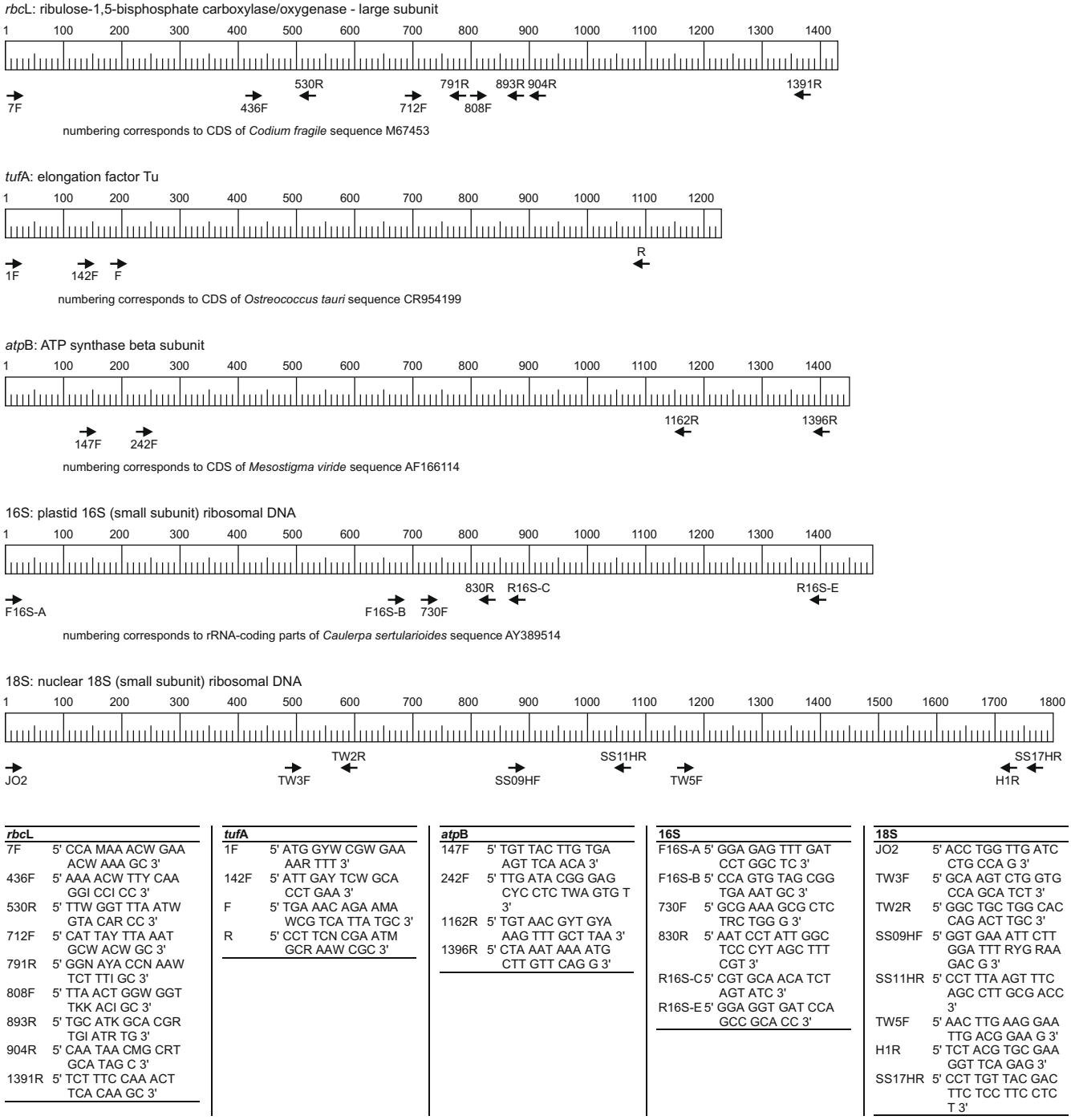

rbcL	
7F	5' CCA MAA ACW GAA ACW AAA GC 3'
436F	5' AAA ACW TTY CAA GGI CCI CC 3'
530R	5' TTW GGT TTA ATW GTA CAR CC 3'
712F	5' CAT TAY TTA AAT GCW ACW GC 3'
791R	5' GGN AYA CCN AAW TCT TTI GC 3'
808F	5' TTA ACT GGW GGT TKK ACI GC 3'
893R	5' TGC ATK GCA CGR TGI ATR TG 3'
904R	5' CAA TAA CMG CRT GCA TAG C 3'
1391R	5' TCT TTC CAA ACT TCA CAA GC 3'

tufA	
1F	5' ATG GYW CGW GAA AAR TTT 3'
142F	5' ATT GAY TCW GCA CCT GAA 3'
F	5' TGA AAC AGA AMA WCG TCA TTA TGC 3'
R	5' CCT TCN CGA ATM GCR AAW CGC 3'

atpB	
147F	5' TGT TAC TTG TGA AGT TCA ACA 3'
242F	5' TTG ATA CGG GAG CYC CTC TWA GTG T 3'
1162R	5' TGT AAC GYT GYA AAG TTT GCT TAA 3'
1396R	5' CTA AAT AAA ATG CTT GTT CAG G 3'

16S	
F16S-A	5' GGA GAG TTT GAT CCT GGC TC 3'
F16S-B	5' CCA GTG TAG CGG TGA AAT GC 3'
730F	5' GCG AAA GCG CTC TRC TGG G 3'
830R	5' AAT CCT ATT GGC TCC CYT AGC TTT CGT 3'
R16S-C	5' CGT GCA ACA TCT AGT ATC 3'
R16S-E	5' GGA GGT GAT CCA GCC GCA CC 3'

18S	
JO2	5' ACC TGG TTG ATC CTG CCA G 3'
TW3F	5' GCA AGT CTG GTG CCA GCA TCT 3'
TW2R	5' GGC TGC TGG CAC CAG ACT TGC 3'
SS09HF	5' GGT GAA ATT CTT GGA TTT RYG RAA GAC G 3'
SS11HR	5' CCT TTA AGT TTC AGC CTT GCG ACC 3'
TW5F	5' AAC TTG AAG GAA TTG ACG GAA G 3'
H1R	5' TCT ACG TGC GAA GGT TCA GAG 3'
SS17HR	5' CCT TGT TAC GAC TTC TCC TTC CTC T 3'

Fig. 2. Primers used for amplification of the five loci used in this study.

2.2. Sequence alignment

After removal of introns in the *rbc*L gene (Hanyuda et al., 2000), all sequences were of equal length and their alignment was unambiguous. The *atp*B sequences were of equal length and their alignment was straightforward. The *tuf*A gene was aligned by eye on the basis of the corresponding amino-acid sequences and ambiguous regions were removed. After introns had been removed, the 16S rDNA sequences were aligned using Muscle v. 3.6 using standard parameters (Edgar, 2004). Ambiguous alignment regions were localized by eye and removed. Alignment of 18S rDNA sequences followed an analogous procedure. The insert near the 3′ terminus of the 18S gene of certain Bryopsidales (Durand et al., 2002; Hillis et al., 1998; Kooistra et al., 1999) was removed because it was not present in all taxa and virtually impossible to align among genera. After removal of this region, sequences were aligned with Muscle v. 3.6 and stripped of their ambiguous regions. The concatenated alignment used for analysis is available through TreeBase and www.phycoweb.net.

2.3. Partitioning and model selection

Selection of a suitable partitioning strategy and suitable models for the various partitions used the Bayesian Information Criterion

Table 1
Taxon list with Genbank accessions and voucher numbers (in parentheses). Vouchers are deposited in the Ghent University Herbarium, the US National Herbarium or the Zechman lab herbarium (CSU Fresno).

Taxon	*rbc*L	*tuf*A	*atp*B	16S	18S
Acetabularia acetabulum	AY177738	FJ535854 (HV1287)			Z33461
Acetabularia calyculus		FJ535855 (HV389)			
Acetabularia crenulata	AY177737		FJ539159		Z33460
Acetabularia dentata	AY177739		FJ480413		Z33468
Acetabularia peniculus	AY177743		FJ539163		Z33472
Acetabularia schenkii	AY177744				Z33470
Avrainvillea lacerata	FJ432635 (HV599)	FJ432651 (HV599)		FJ535833 (HV599)	
Avrainvillea nigricans	FJ432636 (HV891)	FJ432652 (HV891)		FJ535834 (HV891)	
Batophora occidentalis	AY177747		FJ539160		Z33465
Batophora oerstedii	AY177748				Z33463
Bornetella nitida	AY177746		FJ480414		Z33464
Bornetella sp.	FJ535850 (LB1029)				
Bryopsidella neglecta	AY004766				
Bryopsis hypnoides	AY942169			AY221722	
Bryopsis plumosa	FJ432637 (HV880)	FJ432653 (HV880)	FJ480417	FJ535835 (HV880)	FJ432630 (HV880)
Caulerpa flexilis	AJ512485	DQ652532			
Caulerpa sertularioides	AY942170	FJ432654 (HV989)		AY389514	AF479703
Caulerpa taxifolia	AJ316279	AJ417939	FJ539164		
Caulerpa verticillata		AJ417967			
Caulerpella ambigua	FJ432638 (TS78)	FJ432655 (TS24)		FJ535836 (TS78)	
Chalmasia antillana			FJ539161		AY165785
Chlorocladus australasicus	AY177750				Z33466
Chlorodesmis fastigiata	FJ432639 (HV102)			FJ535837 (HV102)	AF416396
Codium lineage 1	AB038481	FJ432662 (H0882)		FJ535838 (SD0509370)	
Codium lineage 2	M67453	U09427		U08345	FJ535848 (KZN2K4.1)
Codium lineage 3	EF108086 (DHO2.178)	FJ535856 (KZN2K4.10)		FJ535839 (H0773)	FJ535849 (KZN2K4.10)
Cymopolia spp.	FJ535851 (WP011)				Z33467
Derbesia marina	AF212142				
Derbesia tenuissima	FJ535852 (H0755)	FJ535857 (H0755)			
Dichotomosiphon tuberosus	AB038487				
Flabellia petiolata	FJ432640 (HV1202)			FJ535847 (HV1202)	AF416389
Halicoryne wrightii	AY177745	FJ535858 (HV565)			AY165786
Halimeda discoidea	AB038488	AY826360 (SOC299)	FJ480416		AF407254 (SOC299)
Halimeda gracilis		AM049965 (HV317)			AF407257 (HEC11839)
Halimeda incrassata	AY942167	AM049958 (H0179)			AF407233 (H0179)
Halimeda micronesica		AM049964 (WLS420-02)			AF407243
Halimeda opuntia	AB038489	AM049967 (HV61)			AF407267 (H0484)
Neomeris dumetosa					Z33469
Oltmannsiellopsis viridis	DQ291132	DQ291132	DQ291132	DQ291133	D86495
Ostreobium sp.	FJ535853 (H0753)	FJ535859 (H0753)		FJ535840 (H0753)	
Parvocaulis exigua	AY177740		FJ539162		
Parvocaulis parvula	AY177741				Z33471
Pedobesia spp.	AY004768			FJ535841 (HV1201)	
Penicillus capitatus	FJ432641 (HV338)				AF416404
Penicillus dumetosus	AY942175				AF416406
Pseudendoclonium akinetum	AY835431	AY835432	AY835433	AY835434	DQ011230
Pseudocodium floridanum	AM909692 (NSF.I23)	AM909697 (NSF.I23)			FJ432631 (NSF.I23)
Pseudocodium natalense	AM909693 (KZNb2241)	AM049969 (KZNb2241)		FJ535842 (KZNb2241)	FJ432632 (KZNb2242)
Rhipidosiphon javensis	FJ432644 (DML40134)			FJ535843 (DML40134)	
Rhipilia crassa	FJ432645 (H0748)	FJ432657 (HV738)		FJ535844 (H0748)	
Rhipilia nigrescens	FJ432646 (H0847)	FJ432658 (HV788)			FJ432633 (HV788)
Rhipilia tomentosa	AY942164				
Rhipiliopsis profunda	FJ432647 (DML51973)	FJ432659 (DML51973)		FJ535845 (DML51973)	
Rhipocephalus phoenix	FJ432648 (HV404)			FJ535846 (HV404)	AF416402
Trentepohlia aurea	FJ534608				DQ399590
Tydemania expeditionis	AY942161	FJ432661 (HV873)			FJ432634 (HV873)
Udotea flabellum	AY942166				AF407270
Udotea glaucescens	FJ432650 (H0862)				
Udotea spinulosa	AY942160				
Ulothrix zonata	AF499683				Z47999
Ulva intestinalis	AB097617	AY454399			AJ000040

(BIC) as a selection criterion (e.g., Sullivan and Joyce, 2005). The guide tree used during the entire procedure was obtained by maximum likelihood (ML) analysis of the concatenated data with a JC69 model with rate variation among sites following a discrete gamma distribution with 8 categories (JC69 + Γ_8) inferred with PhyML (Guindon and Gascuel, 2003). All subsequent likelihood optimizations and BIC calculations were carried out with TreeFinder (Jobb et al., 2004). Six alternative partitioning strategies were considered (see Section 3). Per partitioning strategy, six substitution models were optimized with unlinked parameters between partitions and a partition rate multiplier (see Section 3). The partitioning strategy + model combination receiving the lowest BIC score was used in the phylogenetic analyses documented below.

2.4. Phylogenetic analyses

Phylogenetic analyses consisted of Bayesian inference (BI) and maximum likelihood tree searches using the unrooted partitioned model selected using the BIC procedure (Section 2.3). For Bayesian inference, three independent runs, each consisting of four incre-

mentally heated, Metropolis-coupled chains were run for ten million generations using MrBayes v. 3.1.2 (Ronquist and Huelsenbeck, 2003). The default heating factor, priors, proposal mechanisms and other settings were used. Rate heterogeneity among partitions was modeled by using a variable rate prior. Parameter values and trees were saved every thousand generations. Convergence and stationarity of the runs was assessed using Tracer v. 1.4 (Rambaut and Drummond, 2007). An appropriate burn-in value was determined with the automated method proposed by Beiko et al. (2006). Their method was applied to each run individually, with a sliding window of 100 samples. The post-burnin trees from different runs were concatenated and summarized using MrBayes' sumt command.

Maximum likelihood tree searches were carried out with TreeFinder, which allows likelihood tree searches under partitioned models (Jobb et al., 2004). Tree space coverage in the TreeFinder program is low compared to other ML programs. Therefore, an analysis pipeline was created to increase tree space coverage by running analyses from many start trees. First, a set of start trees was created by randomly modifying the guide tree used for model selection by 100 and 200 nearest neighbor interchange (NNI) steps (50 replicates each). Analyses were run from these 100 start trees. The 3 trees yielding the highest likelihood were used as the starting point for another set of NNI modifications of 20 and 50 steps (50 replicates each). A second set of ML searches was run from each of the resulting 300 start trees. The ML tree resulting from this set of analyses was retained as the overall ML solution. The same partitions and models as in the BI analysis were used, with the second-level tree search and proportional partition rates. Branch support was calculated using the bootstrap resampling method (1000 pseudo-replicates). Bootstrap analyses used the same settings but started from the ML tree.

2.5. Relaxed molecular clock

Likelihood ratio tests significantly rejected a strict (uniform) molecular clock for the alignment. Node age estimates were therefore obtained by fitting a relaxed clock model to our molecular data. The assumption of the molecular clock was relaxed by allowing rates of molecular evolution to vary along the tree according to a Brownian motion model (Kishino et al., 2001; Thorne et al., 1998). First, an F84 model with rate variation across sites following a discrete gamma distribution with 20 rate categories was optimized in PAML v.4 (Yang, 2007), using the topology obtained with Bayesian inference from which all but two outgroups were removed (*Trentepohlia* and *Oltmannsiellopsis*). Second, a variance-covariance matrix was built with estbNew from the T3 package (Thorne et al., 1998; http://abacus.gene.ucl.ac.uk/software.html). Finally, node age estimates were obtained by running three independent MCMC chains with the PhyloBayes program (Lartillot et al., 2007) on the variance-covariance matrix, using the lognormal auto-correlated clock model. Sensitivity analyses were carried out to evaluate the impact of some potentially erroneous fossil assignments with chains of 50,000 generations that were sampled every 100th generation. The final analysis consisted of three independent runs of 1,000,000 generations, sampled every 100th generation. Convergence and stationarity of the chains was evaluated by plotting trace files in Tracer v. 1.4 (Rambaut and Drummond, 2007). The fossils used as calibration points are documented in Section 3.

3. Results

3.1. Data exploration

The data compiled for our analyses consisted of 155 sequences. The resulting five-locus data matrix was 51% filled. The *rbc*L gene was best represented (90% filled), followed by 18S rDNA (62%), *tuf*A (49%), 16S rDNA (33%) and *atp*B (20%). After ambiguously aligned parts had been removed, the matrix measured 61 taxa by 5588 characters. The 18S rDNA provided most characters (1555), followed by *rbc*L (1386), 16S rDNA (1327), *tuf*A (804) and *atp*B (516).

The BIC-based model selection procedure selected a model with four partitions and GTR + Γ_8 substitution models for each partition (Table 2). The four partitions were: (1) ribosomal loci: 18S and 16S, (2) first codon positions of *rbc*L, *tuf*A and *atp*B combined, (3) second codon positions of the three genes, and (4) third codon positions of the three genes.

3.2. Phylogeny of the siphonous algae

Different runs of the Bayesian phylogenetic analysis of the five-locus dataset under an unrooted partitioned model rapidly converged onto highly similar posterior distributions. The chains reached convergence after at most 384,000 generations. The anal-

Table 2
Selection of partitioning strategy and model of sequence evolution using the Bayesian Information Criterion (BIC). The log-likelihood, number of parameters and BIC score are listed for various combination of partitioning strategies and models of sequence evolution. Each partition had its own copy of the model of sequence evolution with a separate set of model parameters. Lower BIC values indicate a better fit of the model to the data. The lowest BIC (in boldface) was observed for the partitioning strategy with four partitions (ribosomal DNA and separate codon positions for each gene), and GTR + Γ_8 models applied to each partition.

Model	ln*L*	# par	BIC
Single partition			
F81	−56405.2	122	113863
F81 + Γ_8	−51296.8	123	103655
HKY	−56009.6	123	113080
HKY + Γ_8	−50707.8	124	102486
GTR	−54913.6	127	110923
GTR + Γ_8	−50224.1	128	101553
2 partitions: ribosomal DNA, protein coding			
F81	−55852.3	126	112792
F81 + Γ_8	−50702.4	128	102509
HKY	−55249.8	128	111604
HKY + Γ_8	−49969.8	130	101061
GTR	−54303.0	136	109779
GTR + Γ_8	−49774.3	138	100739
5 partitions: one for each locus (atpB, rbcL, tufA, 16S, 18S)			
F81	−55772.5	138	112736
F81 + Γ_8	−50769.0	143	102772
HKY	−55160.7	143	111555
HKY + Γ_8	−49913.6	148	101104
GTR	−54145.5	163	109697
GTR + Γ_8	−49483.9	168	100417
4 partitions: ribosomal DNA, separate codon positions for protein coding			
F81	−52199.0	134	105554
F81 + Γ_8	−49807.4	138	100805
HKY	−50927.6	138	103046
HKY + Γ_8	−48121.3	142	97468
GTR	−50455.9	154	102241
GTR + Γ_8	**−47763.5**	**158**	**96890**
5 partitions: 16S, 18S, separate codon positions for protein coding			
F81	−52190.9	138	105572
F81 + Γ_8	−49798.1	143	100830
HKY	−50918.0	143	103070
HKY + Γ_8	−48109.4	148	97496
GTR	−50160.4	163	101727
GTR + Γ_8	−47769.0	168	96988
11 partitions: 16S, 18S, separate codon positions for each gene			
F81	−52087.6	162	105573
F81 + Γ_8	−49742.6	173	100978
HKY	−50825.1	173	103143
HKY + Γ_8	−48071.9	184	97731
GTR	−50188.9	217	102250
GTR + Γ_8	−47561.4	228	97090

yses resulted in a well-resolved phylogenetic hypothesis of the siphonous green algae (Fig. 3A). The backbone of the dasycladalean clade was determined with high confidence except for the branching order between the *Bornetella* lineage, the *Cymopolia-Neomeris* clade and the Polyphysaceae. Relationships among *Acetabularia* species are not resolved with our dataset. In the Bryopsidales, three main clades were inferred, two of which correspond to previously described suborders (Bryopsidineae and Halimedineae). A third lineage contained only the limestone-boring genus *Ostreobium*. Relationships among the three families of the Bryopsidineae were inferred with high confidence (Fig. 3B) whereas within the Halimedineae, relationships among what we will refer to as the "core Halimedineae" (families Caulerpaceae, Rhipiliaceae, Halimedaceae, Pseudocodiaceae and Udoteaceae) remained poorly resolved (Fig. 3C).

3.3. Time-calibrated phylogeny

We compiled a list of fossils that are thought to represent early records of lineages observed in our phylogenetic tree (Table 3). Prior to carrying out the main calibration analysis, we ran several analyses to test the sensitivity of results to the choice of certain fossils as calibration points and of the maximum age constraint imposed on the root of the siphonous algae. The exact combination of constraints used in these trial runs can be found in the online appendix.

Analyses with *Dimorphosiphon* (min. 460.9 my) constrained at node f resulted in considerably older node age estimates throughout the tree than analyses in which this constraint was not imposed. *Dimorphosiphon* has been regarded as an ancestral taxon of the Halimedineae (Dragastan et al., 2002) but its combination of characters did not allow unambiguous placement on any node of the tree. From the incompatibility of this calibration point with the others, we concluded that our admittedly speculative assignment of this taxon to node f was unjustified. With *Dimorphosiphon* excluded from analyses, various combinations of the remaining calibration points led to very similar results.

The analysis was sensitive to the maximum age constraint imposed on the phylogeny. By default, we used a maximum age constraint of 635 my on the root of the siphonous algae (node a) because there is no clear evidence for either Bryopsidales or Dasycladales in Ediacaran Konservat-Lagerstätten, in which macroalgae are abundant and well preserved (Xiao et al., 2002; Zhang et al., 1998). These deposits do, however, contain simple cylindrical and spherical forms (e.g., *Sinospongia*, *Beltanelliformis*) that may be ancestral to these extant lineages (Xiao et al., 2002). Changing the maximum age constraint to 800 my as a sensitivity experiment increased average node ages and widened their 95% confidence intervals. Analogously, lowering the maximum age constraint to 500 my decreased the average ages and narrowed the confidence intervals. The chronogram presented in Fig. 4 resulted from the analysis without *Dimorphosiphon* and with a maximum age constraint of 635 my; more specifically, the analysis was carried out with calibration points a1, a2, b1, c, d2, e1 and h1 (Table 3). Repeating this analysis without age constraint on node b resulted in a chronogram that was very similar.

As an alternative strategy to using a maximum age constraint on the root of the siphonous algae (node a), we constrained the age of node b to be Early Devonian (416.0–397.5 my) based on the first occurrence of fossils with thalli comparable to those of Dasycladaceae, in terms of both general thallus form and reproductive structures, in strata of this age (*Uncatoella*: Kenrick and Li, 1998). This analysis, which is illustrated in the online appendix, should be regarded as a conservative alternative to the analysis presented in Fig. 4 and node ages in this chronogram should be interpreted as minimum values rather than realistic estimates. We will use the chronogram in Fig. 4 as the preferred reference timeframe for the remainder of the paper because the maximum age constraint used for this analysis has an empirical basis (although it is based on absence of evidence rather than evidence of absence) and because we consider the intermediate-sized confidence intervals on the node ages of this tree to yield a fairly realistic image of the true uncertainty surrounding the node ages. In what follows, we report node age estimates as the mean node age followed by the 95% confidence interval in square brackets.

The origin of the orders Dasycladales and Bryopsidales was inferred to be in the Neoproterozoic (571 my [628–510]). The earliest divergence between extant Dasycladaceae lineages occurred during the Ordovician or Silurian (458 my [517–407]) and the family diversified into its main extant lineages during the Devonian. The Polyphysaceae originated from the Dasycladaceae during the second half of the Paleozoic (367 my [435–306]). In the Bryopsidales, the suborders Bryopsidineae and Halimedineae diverged from each other in the Early Paleozoic (456 my [511–405]) and diversified into their component families during the second half of the Paleozoic. The families belonging to the core Halimedineae appear to have diverged from one another during the Permian.

4. Discussion

4.1. Taxonomic implications

The increased sampling of taxa and loci compared to previous studies has produced some results that deserve mention from a taxonomic viewpoint. First, the lineage leading to the limestone-boring genus *Ostreobium* seems to deserve recognition at the suborder level, hence the tentative clade name Ostreobidineae. The bryopsidalean family Udoteaceae disintegrates. Besides the transfer of *Avrainvillea* and *Cladocephalus* to the Dichotomosiphonaceae, which was previously indicated by Curtis et al. (2008), a number of *Rhipilia* and *Rhipiliopsis* species form a lineage of their own and the remainder of the Udoteaceae receives little statistical phylogenetic support. We have applied the name Rhipiliaceae to the clade of *Rhipilia* and *Rhipiliopsis* species. This family name was proposed earlier but its phylogenetic relevance had not yet been demonstrated (Dragastan and Richter, 1999; Dragastan et al., 1997). The same authors proposed the family Avrainvilleaceae to harbor the extant genera *Avrainvillea* and *Cladocephalus* and some fossil genera. However, the ultrastructural affinities between *Dichotomosiphon*, *Avrainvillea* and *Cladocephalus* (Curtis et al., 2008) and the limited DNA sequence divergence between *Dichotomosiphon* and *Avrainvillea* shown here suggest that transferring *Avrainvillea* and *Cladocephalus* to the Dichotomosiphonaceae would be more appropriate. Although the fossil taxa in the Avrainvilleaceae are more difficult to evaluate because no ultrastructural evidence is available to link them unequivocally to the Dichotomosiphonaceae, we nevertheless propose their transfer to this family for taxonomic convenience. We refrain from formally describing a suborder Ostreobidineae for *Ostreobium* because we feel that the description of such high-level taxa should be accompanied by detailed ultrastructural observations.

Our results for the phylogeny of the Dasycladales are consistent with previous studies and do not add much insight into their pattern of diversification. One thing worth mentioning is that the close relationship between *Batophora* and *Chlorocladus*, which was suggested by previous molecular phylogenetic studies (Olsen et al., 1994; Zechman, 2003), is confirmed by our multi-locus dataset. As reported in the aforementioned papers, this finding contradicts the traditional tribe-level classification by Berger and Kaever (1992).

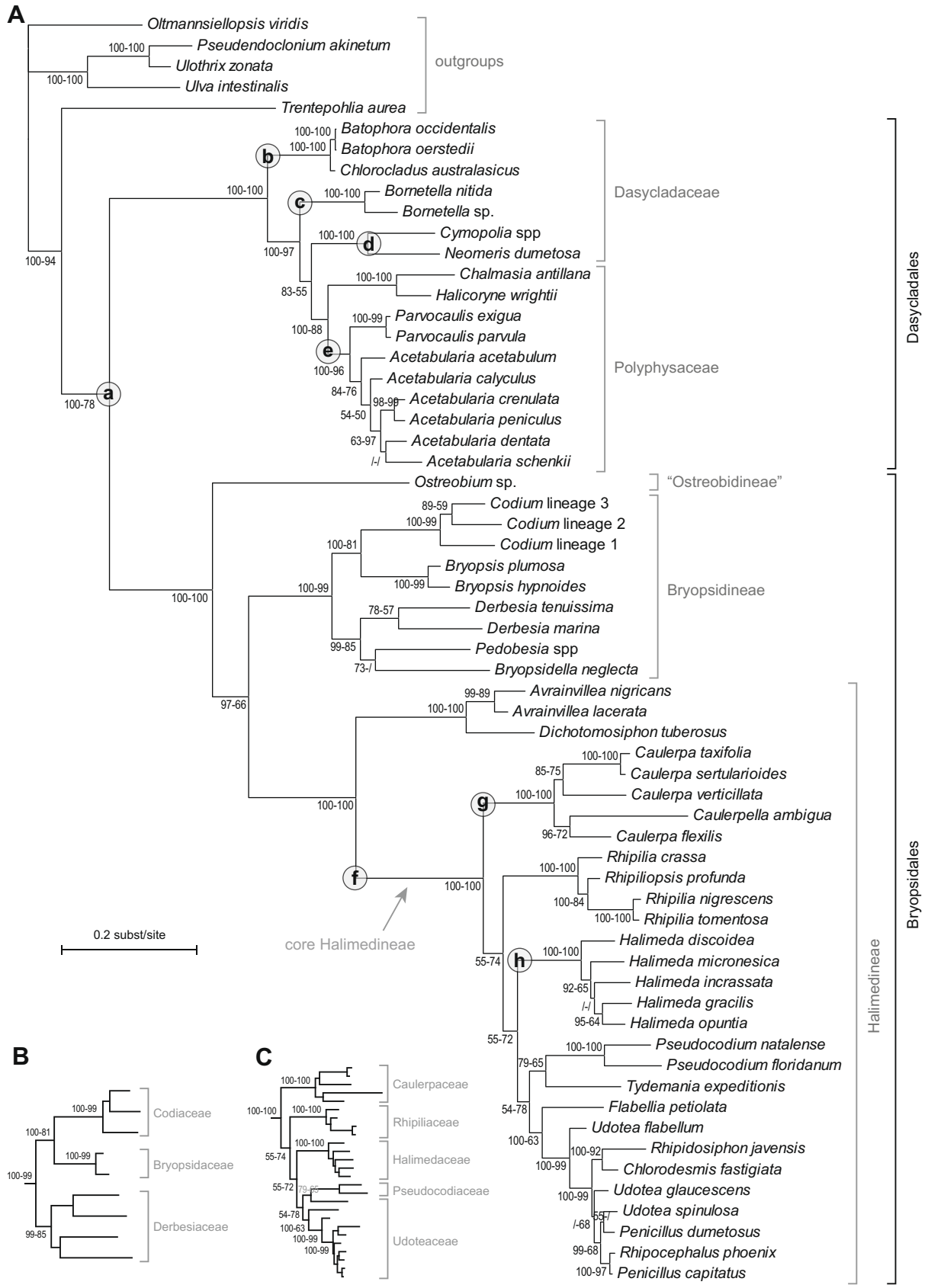

Fig. 3. Phylogenetic relationships among the siphonous green algae inferred from a five-locus DNA alignment using Bayesian analysis under a partitioned, unrooted model. (A) Majority-rule consensus phylogram of post-burnin trees. (B) Relationships among families of the Bryopsidineae. (C) Relationships among families of the core Halimedineae. Numbers at nodes indicate statistical support, posterior probabilities before the dash and ML bootstrap proportions after (both given as percentages). Encircled letters indicate calibration points (Table 3). The scale bar only applies to (A).

Table 3
List of calibration points used to date the phylogenetic tree. The nodes to which the age constraints are applied (first column) are indicated on the phylogram in Fig. 3. If more than one age constraint was identified for a node, these are listed as different calibrations (e.g., calibrations a1, a2 and a3 all apply to node a). The 'age' column indicates the type of constraint (minimum vs. maximum) and the value of the constraint (in million years). Ages of epochs and stages follow the International Stratigraphic Chart (ICS, 2008).

Node	Name	Calibration	Fossil	Period	Age (my)	Reference
a	Siphonous algae crown	a1	Absence of siphonous fossils	Ediacaran	Max 635	Zhang et al. (1998)
		a2	*Yakutina aciculata*	Middle Cambrian	Min 499	Kordé (1957)
		a3	*Chaetocladus plumula*	Middle Ordovician	Min 460.9	Whitfield (1894)
b	Batophoreae stem	b1	*Uncatoella verticillata*	Lower Devonian	Min 397.5	Kenrick and Li (1998)
		b2	*Archaeobatophora typa*	Upper Ordovician	Min 443.7	Nitecki (1976)
		b3	*Uncatoella verticillata*	Lower Devonian	Max 416.0	Kenrick and Li (1998)
c	Bornetelleae stem	c	*Zittelina hispanica*	Hauterivian	Min 130.0	Masse et al. (1993)
d	Neomereae crown	d1	*Neomeris cretacea*	Albian	Min 99.6	Granier and Deloffre (1993)
		d2	*Neomeris cretacea*	Barremian	Min 125.0	Sotak and Misik (1993)
		d3	*Pseudocymopolia jurassica*	Portlandian	Min 142.0	Dragastan (1968)
e	Acetabularieae stem	e1	*Acicularia heberti*	Danian	Min 61.1	Morellet and Morellet (1922)
		e2	*Acicularia boniae*	Middle Triassic	Min 228.7	Iannace et al. (1998)
f	core Halimedineae stem	f	*Dimorphosiphon rectangulare*	Middle Ordovician	Min 460.9	Hoeg (1927)
g	Caulerpaceae stem	g	*Caulerpa* sp.	Wolfcampian	Min 280.0	Gustavson and Delevoryas (1992)
h	Halimeda stem	h1	*Halimeda marondei*	Norian	Min 203.6	Flügel (1988)
		h2	*Halimeda soltanensis*	Upper Permian	Min 251.0	Poncet (1989)

4.2. Dasycladalean diversification

Of the five dasycladalean families, only Dasycladaceae and Polyphysaceae have recent representatives and Seletonellaceae, Triploporellaceae and Diploporellaceae are entirely extinct (Berger and Kaever, 1992). The Seletonellaceae includes the oldest fossils assigned to Dasycladales, *Yakutina aciculata* from the Middle Cambrian (Kordé, 1973; Riding, 1994, 2001) and *Seletonella mira* from the Upper Cambrian (Kordé, 1950b; Riding, 1994, 2001). *Cambroporella* from the Lower Cambrian of Tuva, was initially described as a dasyclad (Kordé, 1950a) but was reinterpreted as a probable bryozoan (Elias, 1954). Unlike living dasyclads, Seletonellaceae contained gametes within the main axis (endospore reproduction) as opposed to within gametophores (sensu Dumais and Harrison, 2000), and developed laterals irregularly along the length of the main axis (aspondyl structure), rather than in whorls as is the case in living representatives (euspondyl structure). Nonetheless, two lines of evidence support a dasyclad affinity for the Seletonellaceae. First, in terms of reproduction, development of reproductive cysts within the main axis is known as a teratology among living dasyclads (Valet, 1968) and all living dasyclads pass through an "endospore stage" as swarms of haploid secondary nuclei generated by meiosis of the large primary nucleus in the rhizoid migrate upward through the main axis towards the gametophores (Berger and Kaever, 1992; Elliott, 1989). Second, an aspondyl structure is a predicted outcome of a detailed reaction-diffusion model of dasyclad whorl morphogenesis (Dumais and Harrison, 2000).

Our chronogram suggests a late Neoproterozoic origin for the Dasycladales, with the 95% confidence interval ranging into the Cambrian: 571 my [628–510] (Fig. 4). The upper boundary on this node age (628 my) should not be overinterpreted because it is largely determined by the upper age constraint on this node (635 my). The Middle Cambrian lower boundary on this node age (510 my), however, can be taken as a fairly safe minimum age estimate for the Dasycladales as well as the Bryopsidales. Unlike *Yakutina* and *Seletonella*, most early Paleozoic dasyclad taxa did not biomineralize (LoDuca et al., 2003). This fact, when taken together with the results of the present analysis, suggests that non-calcified dasyclads may yet be discovered within Konservat-Lagerstätten of latest Neoproterozoic or Early Cambrian age.

Taxa assigned to Dasycladales are both abundant and diverse in Ordovician strata, and include euspondyl (e.g., *Chaetocladus*) as well as aspondyl (e.g., *Dasyporella*) forms (Berger and Kaever, 1992; LoDuca, 1997; LoDuca et al., 2003). The earliest euspondyl forms, like aspondyl taxa, were endospore. Later, however, at least one lineage of euspondyl forms emerged in which gametogenesis occurred within the laterals (cladospore reproduction). Collectively, endospore and cladospore taxa with a euspondyl structure comprise the family Triploporellaceae (Berger and Kaever, 1992; LoDuca, 1997). Triploporellaceae are though to have originated from the Seletonellaceae, indicating that the latter is a paraphyletic group.

The family Dasycladaceae is characterized by euspondyl thalli with spherical gametophores along the sides or tips of laterals (choristospore reproduction). It is though to have originated from the Triploporellaceae, in which case the latter group, like Seletonellaceae, is paraphyletic. Studies indicate that the dasycladacean gametophore, rather than being a modified lateral, is instead a separate structure with its own morphogenetic identity (Dumais and Harrison, 2000). The oldest taxon with gametophores and associated reproductive cysts comparable to those of living Dasycladaceae is *Uncatoella verticillata* from the Lower Devonian (416–397 my) of China (Kenrick and Li, 1998). This taxon is somewhat problematic, however, in that the asymmetrical manner of lateral branching and instances of pseudodichotomies of the main axis are otherwise unknown among dasyclads (Kenrick and Li, 1998). *Uncatoella* is the only taxon known from Paleozoic strata with gametophores and associated reproductive cysts comparable to those of living Dasycladaceae.

Our molecular results suggest that the earliest divergence between the extant Dasycladaceae lineages occurred during the Ordovician or Silurian (458 my [517–407]). Notably, this result emerges regardless of whether *Uncatoella* is used to constrain the minimum age of node b. *Archaeobatophora*, from the Upper Ordovician of Michigan (Nitecki, 1976), is of interest in this regard, as it bears a striking resemblance to the vegetative thallus of the extant dasycladacean *Batophora*. However, gametophores are not present among the few known specimens (all on a single small slab), and thus the status of this form as an early dasycladacean remains uncertain. Our results suggest that the main extant lineages belonging to the Dasycladaceae originated during the Devonian. This is somewhat older than expected because, with the possible exception of the Batophoreae (*Archaeobatophora*), the oldest fossils assigned to extant tribes within the Dasycladaceae are from the Mesozoic (Berger and Kaever, 1992). Similarly, the age estimate for the split between *Cymopolia* and *Neomeris*, two calcified genera known from numerous occurrences in the fossil record, is somewhat older than anticipated: 211 my [300–152] vs. a Barremian age for the earliest *Neomeris* fossil (130–125 my) (Sotak and Misik, 1993). Two factors could explain these discrepancies. First, it is

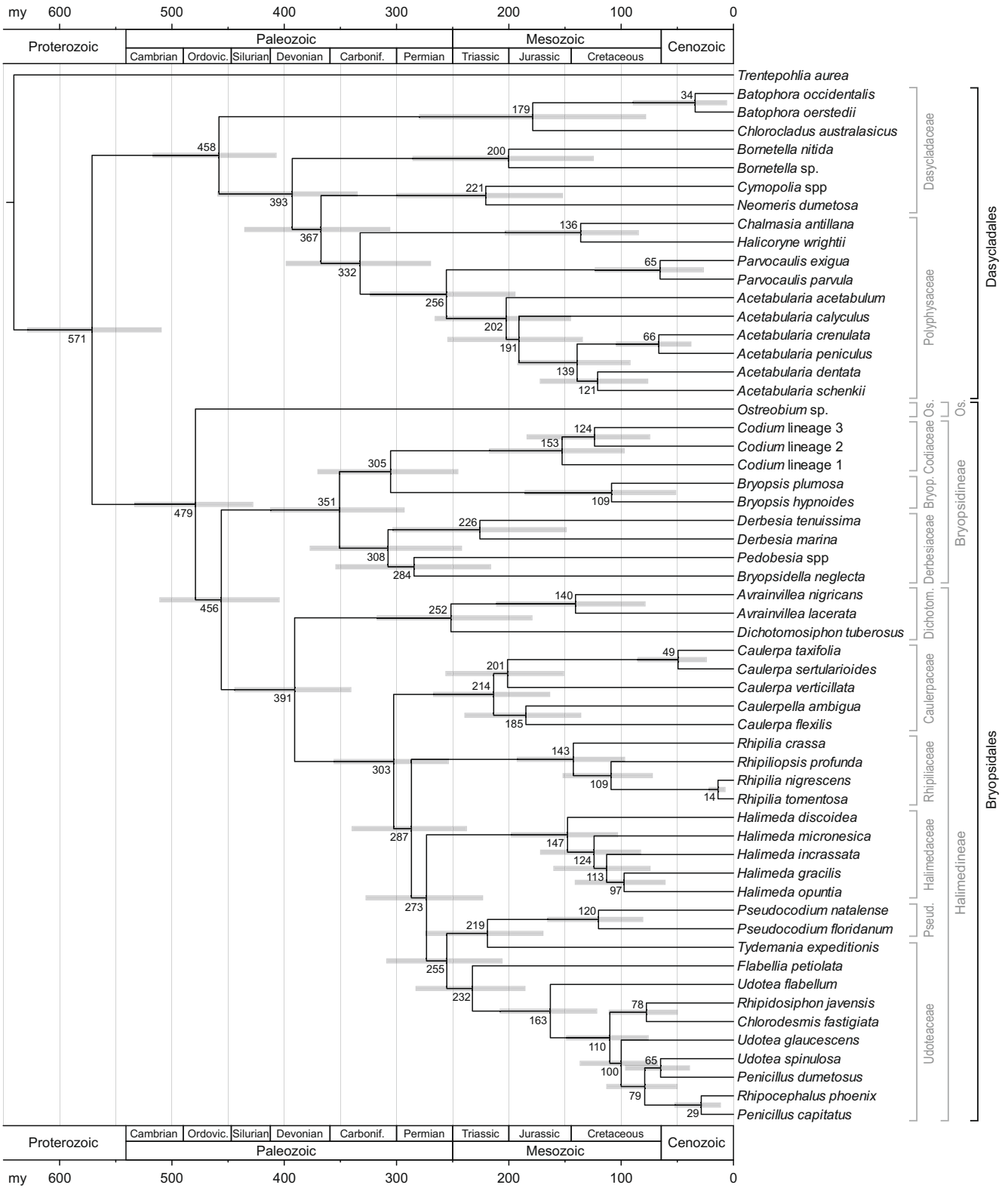

Fig. 4. Chronogram of the siphonous green algae. Node ages were inferred using Bayesian inference assuming a relaxed molecular clock and a set of node age constraints derived from the fossil record. Values at nodes indicate average node ages and bars represent 95% confidence intervals. The calibration points used for this analysis are a1, a2, b1, c, d2, e1 and h1 (Table 3).

possible that many early Dasycladaceae did not biomineralize. This is certainly true for most early Triploporellaceae and Selenonellaceae (LoDuca et al., 2003), and applies to *Uncatoella* and several living Dasycladaceae as well (e.g., *Batophora*). The lack of biomineralization would have severely limited the preservation potential of these taxa. Second, it may be that some Paleozoic and early Mesozoic calcified taxa previously inferred on the basis of lateral morphology to have been endospore or cladospore were in fact choristospore. A choristospore condition for such forms could be masked if calcification was restricted to the outermost

part of the thallus, beyond the level of the gametophores, as is known for the living taxon *Bornetella*.

The family Polyphysaceae is characterized by the development of clavate gametophores arranged in whorls (Berger et al., 2003; Berger and Kaever, 1992). The distinctive gametophores of this group appear to have originated through modification of the spherical gametophores of Dasycladaceae (Dumais and Harrison, 2000). Our results suggest that the Polyphysaceae originated and began their diversification in the second half of the Paleozoic. An Early Carboniferous origin of the family had been suggested based on the fossil taxon *Masloviporella* (Berger and Kaever, 1992; Deloffre, 1988). *Eoclypeina* and *Clypeina* are taxa classified as polyphysaceans from the Permian and Triassic, respectively (Berger and Kaever, 1992). The extant polyphysacean *Halicoryne* has been reported from the Triassic (Misik, 1987; Tomasovych, 2004). However, because these reports are based solely on isolated reproductive elements, both the genus- and family-level assignment of this material must be regarded as tentative (Barattolo and Romano, 2005).

According to the molecular clock results, the polyphysacean taxon *Acetabularia* originated as early as the early Mesozoic. The oldest *Acetabularia* fossils, however, are from the Oligocene (Berger and Kaever, 1992). Here, too, this discrepancy may reflect poor representation of the group in the fossil record, as living members of the genus are only very weakly calcified. Material from Mesozoic-age strata has been assigned to the closely related extant taxon *Acicularia* (Iannace et al., 1998). As is the case for reports of *Halicoryne* from the Triassic, however, such an assignment must be regarded as equivocal because the material at hand comprises only isolated reproductive elements (Barattolo and Romano, 2005).

Overall, the results of the relaxed molecular clock analysis line up rather well against major aspects of dasyclad evolution inferred from the dasyclad fossil record. Nonetheless, our results indicate that the fossil record of certain aspects of the evolutionary history of the Dasycladaceae may be more incomplete than previously suspected (see Kenrick and Li, 1998). The node age estimates obtained in our relaxed molecular clock analysis are older than those recovered by Olsen et al. (1994). Causes for this discrepancy are difficult to pinpoint because differences between the studies are manifold: the molecular clock method, calibration technique, molecular dataset and selection of fossils all differ. Whereas the previous study relied exclusively on 18S rDNA sequences, our dataset includes several additional loci, which should yield more reliable results (Magallón and Sanderson, 2005). Furthermore, at the time the previous study was published, only uniform (strict) molecular clock methods were available. Based on our alignment, 18S rDNA violates the uniform molecular clock (LRT: $-2\,\Delta\ln L = 399.403$, $p < 0.0001$), a statement also true for the other loci in our dataset. As a consequence, node age estimates from our analysis with relaxed molecular clock models should match the true divergence times more closely. The calibration method differs in that fossils are used as minimum age estimates for stem groups in our analyses, whereas they were used as point estimates to determine the rate of 18S rDNA evolution in Olsen et al. (1994). Finally, we use a more extensive list of fossil calibration points, including some recently described fossils that represent older occurrences of some dasyclad clades. Several of the aspects mentioned above would predict our age estimates to be older than those of Olsen et al. (1994), which is in agreement with the empirical results.

4.3. Bryopsidalean diversification

The fossil record of the Bryopsidales is not as well characterized as that of the Dasycladales. Many fossil taxa that are generally considered to belong to the order have been described (reviewed by Bassoullet et al., 1983; Dragastan et al., 1997; Dragastan and Schlagintweit, 2005), but the taxonomic placement of these taxa is often ambiguous (Mu, 1990). Dragastan and Schlagintweit (2005) presented an evolutionary scenario of bryopsidalean diversification based on their interpretation of calcified fossil taxa. They proposed a temporal succession of three main lineages. The primitive Dimorphosiphonaceae, characterized by a single medullar siphon and a simple cortex, originated in the Neoproterozoic or early Paleozoic and persisted through the Devonian (±360 my). The Protohalimedaceae, characterized by multiple medullar siphons and a cortex of variable complexity, diverged from the Dimorphosiphonaceae in the early Silurian (±440 my) and thrived up to the PT-boundary (±250 my), when it suffered major losses, and continued into the Mesozoic to go extinct during the Cretaceous. The extant family Halimedaceae, which features multiple medullar siphons and a complex cortex, was thought to have diverged from the Protohalimedaceae in the second half of the Permian (270–250 my) and diversified through the Mesozoic and Cenozoic.

In our opinion, relationships between fossil taxa and lineages in the phylogeny of extant taxa are not evident. This uncertainty is reflected in our study by the lower number of fossil calibration points used within the Bryopsidales. Our time-calibrated phylogeny indicates that after the initial diversification of the order into its suborders during the early Paleozoic, current families originated in the second half of the Paleozoic. It also suggests that calcification is a relatively recent phenomenon in the extant lineages of the Bryopsidales because the Halimedaceae and Udoteaceae, the only extant families with calcified, corticated representatives, originated during the Permian (±300–250 my) and diversified during the Mesozoic (Fig. 4). All other lineages of the Halimedineae, including some recently discovered lineages (Verbruggen et al., 2009), are not calcified. As a consequence, the presence of the calcified, corticated families Dimorphosiphonaceae and Protohalimedaceae in older deposits is difficult to interpret in the context of our phylogeny. Based on our results, the classical paleontological interpretation that the Dimorphosiphonaceae and Protohalimedaceae are direct ancestral forms of the serial-segmented Halimedaceae seems doubtful. First, our phylogenetic results show no indication of the presence of calcification in Bryopsidales prior to the Permian. Second, it follows from our phylogeny that the internal architecture of thalli was relatively simple up until the late Paleozoic. Thalli consisting of a medulla and a cortex appear to have evolved from simple, siphonous thalli several times independently during the Permian–Triassic period. They evolved once in the Bryopsidineae (*Codium*), a second time in the Dichotomosiphonaceae (*Avrainvillea*) and a third time in the core Halimedineae (Halimedaceae, Udoteaceae and Pseudocodiaceae).

Some alternative hypotheses may be posited to explain this disparity of results, all of which should be regarded as speculative. Assuming that the Dimorphosiphonaceae and Protohalimedaceae are genuine Bryopsidales, these two families could very well represent an early-diverging bryopsidalean lineage that went extinct. Alternatively, they could represent a collection of taxa that branched off at various places along the lineage leading from the origin of the Halimedineae to the Halimedaceae and Udoteaceae.

4.4. Perspectives

The genera *Codium* and *Halimeda* have been proposed as model systems for studying marine algal speciation, biogeography and macroevolution (Kooistra et al., 2002; Verbruggen et al., 2007). Both these genera are species-rich, ecologically diverse and geographically widespread, making them ideal case studies for a spectrum of evolutionary questions. Furthermore, these genera contrast in their climatic preferences, *Halimeda* being mostly tropical and *Codium* being more diverse in temperate seas. Further development of these case studies will greatly benefit from the

temporal framework provided here. Both genera diverged from their respective sister lineages in the late Paleozoic (*Halimeda*: 273 my [327–223]; *Codium*: 307 my [370–245]). The most recent common ancestor of the extant species in both genera are highly comparable and can be situated in the Late Jurassic—Early Cretaceous (*Halimeda*: 147 my [198–103]; *Codium*: 153 my [217–97]). To get an initial idea of the timeframe of evolutionary diversification we have included representatives of each of the five sections of *Halimeda* (Verbruggen and Kooistra, 2004) and each of the three major lineages of *Codium* (Verbruggen et al., 2007). It follows from our results that both genera spawned their major extant lineages during the Cretaceous. This close match between the timeframes of evolutionary diversification of both genera is convenient for comparative studies between them.

One advantage of using the calcified genus *Halimeda* as a model for marine evolution is that phylogenetic results can be contrasted with its extensive fossil record. An initial comparison of our results to interpretations of the fossil record marks a different timeframe of diversification: whereas the fossil record suggests diversification of the genus into its main lineages (taxonomic sections) in the Eocene (roughly 56–34 my) (Dragastan and Herbig, 2007), our results indicate a considerably older, Cretaceous divergence (between approximately 147 and 97 my). The contradiction of these results cannot be explained at present, but three hypotheses are suggested. First, a deviation of the true molecular evolutionary process from the relaxed molecular clock model used here could cause the contradiction. Second, misinterpretation of the fossil record used to calibrate our tree may be at the basis. Third, a significant gap could be present in the fossil record. To distinguish between these alternative scenarios, additional paleontological as well as molecular phylogenetic research is needed. Paleontologists should document additional time-series in the fossil record, especially through the Cretaceous and Paleogene systems (145–23 my). Molecular systematists should evaluate the fit of different clock relaxation models to the molecular data (e.g., Lepage et al., 2007) and take different calibration approaches, either top-down (as was done here) or bottom-up (from calibration points within the genus).

The literature on the genus *Halimeda* is marked by a contradiction of species ages inferred from paleontological and molecular phylogenetic data. In the paleontological literature, extant species are commonly reported from Miocene (>5 my) and Paleogene deposits (>23 my), and some are even thought to date back to the Triassic (>200 my) (Dragastan and Herbig, 2007; Dragastan et al., 2002). In contrast, interpretation of vicariance patterns in molecular phylogenetic trees implied that extant species were younger than 3 my, and reports of extant species in the fossil record were interpreted as the result of iterative convergent evolution (Kooistra et al., 2002). Because of this possibility, we have not used any calibration points within the genus; only its earliest appearance was used to calibrate the clock. Even though the present study was not designed to answer questions about species ages in *Halimeda*, we can glean some information from its results. These indicate that the five sections of *Halimeda* diverged from one another during the first half of the Cretaceous (between approximately 147 and 97 my). Because each of the sections diversified relatively soon after they originated, we conclude that species ages must be considerably older than implied by Kooistra et al. (2002). This result also implies that the iterative morphological convergence hypothesis should be re-evaluated. It should be clear that we do not imply that the hypothesis is false, and records of extant species in Miocene and older sediments should certainly not be accepted without scrutiny. For example, Dragastan et al. (2002) synonymized several Mesozoic taxa, including some Triassic ones (>200 my) with the extant taxon *H. cylindracea* because of similar segment shape. It follows directly from our results that no extant species can be of Triassic age and we are of the opinion that using extant species as form taxa for fossils is undesirable. Comparative studies of extant taxa in a molecular phylogenetic framework have presented unambiguous evidence that morphological convergence, especially of segment shape, has occurred during *Halimeda* evolution (Kooistra et al., 2002; Verbruggen et al., 2005). Consequently, interpretation of fossils as extant species should follow only from statistically sound morphometric analyses, preferably using time-series in various parts of the world.

Acknowledgments

We thank Fabio Rindi and Juan Lopez-Bautista for providing a *Trentepohlia rbc*L sequence. We are grateful to Barrett Brooks, Roxie Diaz, Cristine Galanza, John Huisman, Gerry Kraft, Tom and Courtney Leigh, Dinky Olandesca, Tom Schils and John West for collecting specimens or providing assistance in the field. We thank Fabio Rindi and an anonymous referee for their constructive comments on a previous version of the manuscript. Funding was provided by FWO-Flanders (research Grant G.0142.05, travel grants and post-doctoral fellowships to H.V. and F.L.), NSF (DEB-0128977 to F.W.Z.), the Ghent University BOF (doctoral fellowship to E.C. and travel grant to F.W.Z.), the Smithsonian Marine Station at Fort Pierce, Florida (SMS Contribution 760), the Flemish Government (bilateral research Grant 01/46) and the King Leopold III Fund for Nature Exploration and Conservation.

Appendix A. Supplementary data

Supplementary data associated with this article can be found, in the online version, at doi:10.1016/j.ympev.2008.12.018.

References

Barattolo, F., Romano, R., 2005. Shallow carbonate platform bioevents during the Upper Triassic–Lower Jurassic: an evolutive interpretation. Boll. Soc. Geol. Ital. 124, 123–142.

Bassoullet, J.P., Bernier, P., Deloffre, R., Genot, P., Poncet, J., Roux, A., 1983. Les algues Udoteacées du Paléozo au Cénozo. Bull. Centr. Rech. Expl.—Prod. Elf Aquitaine 7, 449–621.

Beiko, R.G., Keith, J.M., Harlow, T.J., Ragan, M.A., 2006. Searching for convergence in phylogenetic Markov chain Monte Carlo. Syst. Biol. 55, 553–565.

Berger, S., 2006. Photo-atlas of living Dasycladales. Carnets de Géologie/Notebooks on Geology 2, 1–348.

Berger, S., Fettweiss, U., Gleissberg, S., Liddle, L.B., Richter, U., Sawitzky, H., Zuccarello, G.C., 2003. 18S rDNA phylogeny and evolution of cap development in Polyphysaceae (formerly Acetabulariaceae; Dasycladales, Chlorophyta). Phycologia 42, 506–561.

Berger, S., Kaever, M.J., 1992. Dasycladales: an illustrated monograph of a fascinating algal order. Thieme, Stuttgart.

Bucur, I.I., 1999. Stratigraphic significance of some skeletal algae (Dasycladales, Caulerpales) of the Phanerozoic. In: Farinacci, A., Lord, A.R. (Eds.), Depositional Episodes and Bioevents. Università La Sapienza, Rome, pp. 53–104.

Curtis, N.E., Dawes, C.J., Pierce, S.K., 2008. Phylogenetic analysis of the large subunit rubisco gene supports the exclusion of *Avrainvillea* and *Cladocephalus* from the Udoteaceae (Bryopsidales, Chlorophyta). J. Phycol. 44, 761–767.

Deloffre, R., 1988. Nouvelle taxonomie des algues Dasycladales. Bull. Centr. Rech. Expl.—Prod. Elf Aquitaine 12, 165–217.

Doyle, J.J., Doyle, J.L., 1987. A rapid DNA isolation procedure for small quantities of fresh leaf tissue. Phytochem. Bull. 19, 11–15.

Dragastan, O.N., 1968. Algues calcaires dans le Jurassique superieur de Roumanie. Geologica Romana 7, 59–74.

Dragastan, O.N., Herbig, H.-G., 2007. *Halimeda* (green siphonous algae) from the Paleogene of (Morocco)—taxonomy, phylogeny and paleoenvironment. Micropaleontology 53, 1–72.

Dragastan, O.N., Littler, D.S., Littler, M.M., 2002. Recent vs. fossil *Halimeda* species of Angaur Island, Palau and adjacent western Pacific areas. Acta Palaeontol. Rom., Special publication No. 1.

Dragastan, O.N., Richter, D.K., 1999. Late Jurassic oolites from the Acrocorinth (NE-Peloponnesus): Calcareous micro-algae as an exceptional palaeoecologic indicator. Beiträge zur Sedimentgeologie von Griechenland, 149–172.

Dragastan, O.N., Richter, D.K., Kube, B., Popa, M., Sarbu, A., Ciugulea, I., 1997. A new family of Paleo-Mesozoic calcareous green Siphons-algae (order Bryopsidales, class Bryopsidophyceae, phylum Siphonophyta). Rev. Esp. Micropaleont. 29, 69–135.

Dragastan, O.N., Schlagintweit, F., 2005. Mesozoic algae of family Protohalimedaceae Dragastan, Littler & Littler, 2002 (Chlorophycota): a critical review. Acta Palaeontol. Rom. 5, 107–140.
Dumais, J., Harrison, L.G., 2000. Whorl morphogenesis in the dasycladalean algae: the pattern formation viewpoint. Phil. Trans. Roy. Soc. B—Biol. Sci. 355, 281–305.
Durand, C., Manuel, M., Boudouresque, C.F., Meinesz, A., Verlaque, M., Le Parco, Y., 2002. Molecular data suggest a hybrid origin for the invasive *Caulerpa racemosa* (Caulerpales, Chlorophyta) in the Mediterranean Sea. J. Evol. Biol. 15, 122–133.
Edgar, R.C., 2004. MUSCLE: multiple sequence alignment with high accuracy and high throughput. Nucleic Acids Res. 32, 1792–1797.
Elias, M.K., 1954. *Cambroporella* and *Coeloclema*. Lower Cambrian and Ordovician bryozoans. J. Paleontol. 28, 52–58.
Elliott, G.F., 1989. The evidence of reproductive mechanisms in the fossil dasyclads (Algae: Chlorophyta). Biol. Rev. Cambr. Phil. Soc. 64, 269–275.
Famà, P., Wysor, B., Kooistra, W., Zuccarello, G.C., 2002. Molecular phylogeny of the genus *Caulerpa* (Caulerpales, Chlorophyta) inferred from chloroplast *tuf*A gene. J. Phycol. 38, 1040–1050.
Flügel, E., 1988. *Halimeda*: paleontological record and palaeoenvironmental significance. Coral Reefs 6, 123–130.
Granier, B., Deloffre, R., 1993. Inventaire critique des algues Dasycladales fossiles. IIe partie—Les algues Dasycladales du Jurassique et du Crétacé. Rev. Paléobiol. Genève 12, 19–65.
Guindon, S., Gascuel, O., 2003. A simple, fast, and accurate algorithm to estimate large phylogenies by maximum likelihood. Syst. Biol. 52, 696–704.
Guiry, M.D., Guiry, G.M., 2008. AlgaeBase. World-wide electronic publication. http://www.algaebase.org.
Gustavson, T.C., Delevoryas, T., 1992. *Caulerpa*-like marine alga from Permian Strata, Palo Duro basin, West Texas. J. Paleontol. 66, 160–161.
Hanyuda, T., Arai, S., Ueda, K., 2000. Variability in the *rbc*L introns of Caulerpalean algae (Chlorophyta, Ulvophyceae). J. Plant Res. 113, 403–413.
Hillis, L.W., Engman, J.A., Kooistra, W.H.C.F., 1998. Morphological and molecular phylogenies of *Halimeda* (Chlorophyta, Bryopsidales) identify three evolutionary lineages. J. Phycol. 34, 669–681.
Hillis-Colinvaux, L., 1986. Distribution patterns of some Bryopsidales in the geologic past: their bearing on present distributions. Bot. Mar. 29, 271–277.
Hoeg, O.A., 1927. *Dimorphosiphon rectangulare*, a new Codiacea from Ordovician of Norway. Avhandlinger Utgitt av det Norske Videnskaps-Akademi i Oslo. I. Matematisk-Naturvidenskapelig Klasse 4, 1–16.
Iannace, A., Radiocic, R., Zamparelli, V., 1998. A new dasycladalean alga from the Middle Triassic Carbonates of northern Calabria. Facies 39, 67–74.
ICS, 2008. International Stratigraphic Chart (International Commission on Stratigraphy).
Jobb, G., von Haeseler, A., Strimmer, K., 2004. TREEFINDER: a powerful graphical analysis environment for molecular phylogenetics. BMC Evol. Biol. 4, 18.
Karol, K.G., McCourt, R.M., Cimino, M.T., Delwiche, C.F., 2001. The closest living relatives of land plants. Science 294, 2351–2353.
Kenrick, P., Li, C.S., 1998. An early, non-calcified, dasycladalean alga from the Lower Devonian of Yunnan Province. China Rev. Palaeobot. Palyno. 100, 73–88.
Kishino, H., Thorne, J.L., Bruno, W.J., 2001. Performance of a divergence time estimation method under a probabilistic model of rate evolution. Mol. Biol. Evol. 18, 352–361.
Kooistra, W., 2002. Molecular phylogenies of Udoteaceae (Bryopsidales, Chlorophyta) reveal nonmonophyly for *Udotea*, *Penicillus* and *Chlorodesmis*. Phycologia 41, 453–462.
Kooistra, W., Caldéron, M., Hillis, L.W., 1999. Development of the extant diversity in *Halimeda* is linked to vicariant events. Hydrobiologia 398, 39–45.
Kooistra, W., Coppejans, E.G.G., Payri, C., 2002. Molecular systematics, historical ecology, and phylogeography of *Halimeda* (Bryopsidales). Mol. Phylogenet. Evol. 24, 121–138.
Kordé, K.B., 1950a. Algal remains in the Cambrian of the Kazakhstan. Doklady Akademii Nauk SSSR 73, 809–812.
Kordé, K.B., 1950b. Dasycladaceae from the Cambrian of Tuva. Doklady Akademii Nauk SSSR 73, 371–374.
Kordé, K.B., 1957. Nouvelles représentantes des algues siphonées. Akademii Nauk SSSR 1.
Kordé, K.B., 1973. Cambrian algae. Trudy Instituta Paleontologii, Akademiya Nauk SSSR 139, 1–347.
Lam, D.W., Zechman, F.W., 2006. Phylogenetic analyses of the Bryopsidales (Ulvophyceae, Chlorophyta) based on Rubisco large subunit gene sequences. J. Phycol. 42, 669–678.
Lartillot, N., Blanquart, S., Lepage, T., 2007. PhyloBayes. Available from: <http://www.lirmm.fr/mab/article.php3?id_article=329/>.
Lepage, T., Bryant, D., Philippe, H., Lartillot, N., 2007. A general comparison of relaxed molecular clock models. Mol. Biol. Evol. 24, 2669–2680.
LoDuca, S.T., 1997. The green alga *Chaetocladus* (Dasycladales). J. Paleontol. 71, 940–949.
LoDuca, S.T., Kluessendorf, J., Mikulic, D.G., 2003. A new noncalcified dasycladalean alga from the Silurian of Wisconsin. J. Paleontol. 77, 1152–1158.
Lopez-Bautista, J.M., Chapman, R.L., 2003. Phylogenetic affinities of the Trentepohliales inferred from small-subunit rDNA. Int. J. Syst. Evol. Microbiol. 53, 2099–2106.
Magallón, S.A., Sanderson, M.J., 2005. Angiosperm divergence times: the effect of genes, codon positions, and time constraints. Evolution 59, 1653–1670.
Masse, J.-P., Arias, C., Vilas, L., 1993. *Zittelina hispanica* et *Suppiluliumaella minuta*, Dasycladales nouvelles de l'Hauterivien du Sud-Est de l'Espagne. Rev. Micropaleont. 36, 293–300.
Misik, M., 1987. The alga *Halicoryne carpatica* n. Sp. from Upper Triassic of western Carpathians. Geologicky Zbornick—Geologica Carpathica 38, 285–293.
Morellet, L., Morellet, J., 1922. Nouvelle contribution a l'étude des Dasycladacées tertiaires. Mem. Soc. Geol. France, Paleont. 25 (58), 1–35.
Mu, X., 1990. Fossil Udoteaceae and Gymnocodiaceae. In: Riding, R. (Ed.), Calcareous algae and stromatolites. Springer-Verlag, Berlin, pp. 146–166.
Nitecki, M.H., 1976. Ordovician Batophoreae (Dasycladales) from Michigan. Fieldiana Geology 35.
Olsen, J.L., Stam, W.T., Berger, S., Menzel, D., 1994. 18S rDNA and evolution in the Dasycladales (Chlorophyta): modern living fossils. J. Phycol. 30, 729–744.
Olson, K.N., Melton, R.S., Yaudes, K.M., Norwood, K.G., Freshwater, D.W., 2005. Characteristics and utility of plastid-encoded 16S rRNA gene sequence data in phylogenetic studies of red algae. J. North Carolina Acad. Sci. 120, 143–151.
Poncet, J., 1989. Présence du genre *Halimeda* Lamouroux, 1812 (algue verte calcaire) dans Ie Permien supérieur du sud Tunisien. Revue Micropal. 32, 40–44.
Rambaut, A., Drummond, A.J., 2007. Tracer. Available from: <http://beast.bio.ed.ac.uk/tracer/>.
Riding, R., 1994. Evolution of algal and cyanobacterial calcification. In: Bengtson, S. (Ed.), Early Life on Earth. Columbia University Press, New York, pp. 426–438.
Riding, R., 2001. Calcified algae and cyanobacteria. In: Zhuravlev, A., Riding, R. (Eds.), The Ecology of the Cambrian Radiation. Columbia University Press, New York, pp. 445–473.
Ronquist, F., Huelsenbeck, J.P., 2003. MrBayes 3: Bayesian phylogenetic inference under mixed models. Bioinformatics 19, 1572–1574.
Sotak, J., Misik, M., 1993. Jurassic and Cretaceous dasycladalean algae from the eastern Carpathians. Boll. Soc. Paleontol. Ital Spec. 1.
Sullivan, J., Joyce, P., 2005. Model selection in phylogenetics. Ann. Rev. Ecol. Evol. Syst. 36, 445–466.
Thorne, J.L., Kishino, H., Painter, I.S., 1998. Estimating the rate of evolution of the rate of molecular evolution. Mol. Biol. Evol. 15, 1647–1657.
Tomasovych, A., 2004. Microfacies and depositional environment of an Upper Triassic intra-platform carbonate basin: the Fatric Unit of the West Carpathians (Slovakia). Facies 50, 77–105.
Valet, G., 1968. Contribution à l'étude des Dasycladales. 1. Morphogenèse. Nova Hedwigia 16, 21–82.
Verbruggen, H., De Clerck, O., Schils, T., Kooistra, W., Coppejans, E., 2005. Evolution and phylogeography of *Halimeda* section *Halimeda*. Mol. Phylogenet. Evol. 37, 789–803.
Verbruggen, H., Kooistra, W., 2004. Morphological characterization of lineages within the calcified tropical seaweed genus *Halimeda* (Bryopsidales, Chlorophyta). Eur. J. Phycol. 39, 213–228.
Verbruggen, H., Leliaert, F., Maggs, C.A., Shimada, S., Schils, T., Provan, J., Booth, D., Murphy, S., De Clerck, O., Littler, D.S., Littler, M.M., Coppejans, E., 2007. Species boundaries and phylogenetic relationships within the green algal genus *Codium* (Bryopsidales) based on plastid DNA sequences. Mol. Phylogenet. Evol. 44, 240–254.
Verbruggen, H., Theriot, E.C., 2008. Building trees of algae: some advances in phylogenetic and evolutionary analysis. Eur. J. Phycol. 43, 229–252.
Verbruggen, H., Vlaeminck, C., Sauvage, T., Sherwood, A.R., Leliaert, F., De Clerck, O., 2009. Phylogenetic analysis of Pseudochlorodesmis strains reveals cryptic diversity above the family level in the siphonous green algae (Bryopsidales, Chlorophyta). J. Phycol., in press.
Whitfield, R.P., 1894. On new forms of marine algae from the Trenton Limestone with observations of *Buthograptus laxus* Hall. Am. Mus. Nat. Hist. Bull. 6, 351–358.
Wolf, P.G., 1997. Evaluation of *atp*B nucleotide sequences for phylogenetic studies of ferns and other pteridophytes. Am. J. Bot. 84, 1429–1440.
Woolcott, G.W., Knoller, K., King, R.J., 2000. Phylogeny of the Bryopsidaceae (Bryopsidales, Chlorophyta): cladistic analyses of morphological and molecular data. Phycologia 39, 471–481.
Xiao, S.H., Yuan, X.L., Steiner, M., Knoll, A.H., 2002. Macroscopic carbonaceous compressions in a terminal Proterozoic shale: a systematic reassessment of the Miaohe biota, south China. J. Paleontol. 76, 347–376.
Yang, Z., 2007. PAML 4: phylogenetic analysis by maximum likelihood. Mol. Biol. Evol. 24, 1586–1591.
Zechman, F.W., 2003. Phylogeny of the Dasycladales (Chlorophyta, Ulvophyceae) based on analyses of RUBISCO large subunit (*rbc*L) gene sequences. J. Phycol. 39, 819–827.
Zechman, F.W., Theriot, E.C., Zimmer, E.A., Chapman, R.L., 1990. Phylogeny of the Ulvophyceae (Chlorophyta): cladistic analysis of nuclear-encoded ribosomal-RNA sequence data. J. Phycol. 26, 700–710.
Zhang, Y., Yin, L.M., Xiao, S.H., Knoll, A.H., 1998. Permineralized fossils from the terminal Proterozoic Doushantuo Formation, South China. J. Paleontol. 72, 1–52.